Dual–Color Fluorescence and Homogeneous Immunoassay for the Determination of Human Enterovirus 71

8 AUTHORS, INCLUDING:

Zhang Cuiling
East China Normal University
14 PUBLICATIONS **247** CITATIONS

SEE PROFILE

Guohua Zhou
Lingnan Normal University
27 PUBLICATIONS **330** CITATIONS

SEE PROFILE

Zhike He
Wuhan University
144 PUBLICATIONS **2,449** CITATIONS

SEE PROFILE

# Dual-Color Fluorescence and Homogeneous Immunoassay for the Determination of Human Enterovirus 71

Lu Chen,[†] Xiaowei Zhang,[‡] Cuiling Zhang,[†] Guohua Zhou,[†] Wanpo Zhang,[‡] Dongshan Xiang,[†] Zhike He,[*,†] and Hanzhong Wang[‡]

[†]Key Laboratory of Analytical Chemistry for Biology and Medicine (Ministry of Education), College of Chemistry and Molecular Sciences, Wuhan University, Wuhan, 430072, PR China

[‡]State Key Laboratory of Virology, Wuhan Institute of Virology, Chinese Academy of Sciences, Wuhan, 430071, PR China

Ⓢ Supporting Information

ABSTRACT: We have developed a new fluorescent immune ensemble probe comprised of a conjugated lower toxic water-soluble CdTe:Zn^{2+} quantum dots (QDs) and Ru(bpy)$_2$(mcbpy-O-Su-ester)(PF$_6$)$_2$- antibody complex (Ru-Ab) for the dual-color determination of human enterovirus 71 (EV71) in homogeneous solution. EV71 monoantibody was easily covalently conjugated with Ru(bpy)$_2$(mcbpy-O-Su-ester)(PF$_6$)$_2$ to form a stable complex Ru-Ab, which acted both as an effective quencher of QDs fluorescence and the capture probe of virus antigen EV71. Herein, the target EV71 can break up the low fluorescent ionic ensemble by antigen—antibody combination to set free the fluorescent QDs and restore the fluorescence of QDs whereas the fluorescence intensity of Ru-Ab remains the same. Thus, the determination of EV71 by the complex Ru-Ab and QDs can be realized via the restoration of QDs fluorescence upon addition of EV71 and even can be directly evaluated by the ratio of green-colored QDs fluorescence intensity to Ru-Ab red-colored fluorescence intensity. The green-colored fluorescence of QDs was very sensitive to the change of EV71 concentration, and its fluorescence intensity increased with the increase of EV71 concentration between 1.8 ng/mL and 12 μg/mL. With this method, EV71 was detected at subnanogram per milliliter concentration in the presence of 160 μg/mL bovine serum albumin. More importantly, this strategy can be used as a universal method for any protein or virus by changing conjugated antibodies in disease early diagnosis providing a fast and promising clinical approach for virus determination. In a word, a simple, fast, sensitive, and highly selective assay for EV71 has been described. It could be applied in real sample analysis with a satisfactory result. It was notable that the sensor could not only achieve rapid and precise quantitative determination of protein/virus by fluorescent intensity but also could be applied in semiquantitative protein/virus determination by digital visualization.
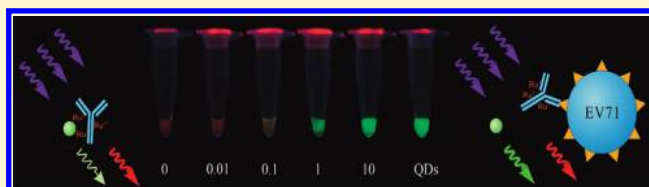
EV71 is the main etiological agent of hand, foot, and mouth disease (HFMD), which is a common childhood exanthema characterized by mild fever, multiple oral ulcers, and papulovesicular rash on the skin of limbs and buttocks. It is associated with neurological complications such as aseptic meningitis, brainstem encephalitis, and poliomyelitis-like paralysis, which have led to severe cases with high mortalities in recent outbreaks in the Asia-Pacific region.[1,2] With the increasing concerns of the fatal HFMD caused by EV71, there is an urgent need for a rapid and specific method to determine the virus for early diagnosis. The classical virus detection technologies usually include virus isolation by cell culture, polymerase chain reaction (PCR), and enzyme-linked immunosorbent assays (ELISA).[3] To the best of our knowledge, the cell culture method requires a long period of time to finish the viral replication course to obtain the quantitative result.[4] Various PCR assays require expensive commercial reagents and sophisticated instruments for routine and large-scale assays or point-of-care detection.[5,6] Classically, the heterogeneous sandwich-type assay format ELISA is applied where capture molecules are being immobilized on modified surfaces and bound targets are detected by secondary antibodies.[7] Nevertheless, heterogeneous assay formats often suffered from false-positive signals that arise from nonspecific surface interactions and are usually labor-intensive. To prevent false-positive signals and improve data quality, homogeneous assay formats are popular alternatives that allow the detection of target molecules by ligand binding interactions in solution as they occur under physiological conditions.[8,9] Therefore, great efforts have been contributed to searching for simple and fast homogeneous models of virus detection.[10,11] More recently, there are many research groups who have developed chemical analytical sensors for virus detection. Lai et al. have fabricated a potentially generalizable electrochemical peptide-based (E-PB) sensor for the detection of HIV.[12] Altug et al provided a proof-of-concept biosensing platform for fast, compact, quantitative, and label-free sensing of viral particles, which opened up a new opportunity for single virus detection.[13]

Scheme 1. Schematic Illustration of the QDs and Ru-Ab Complex Based EV71 Biosensor
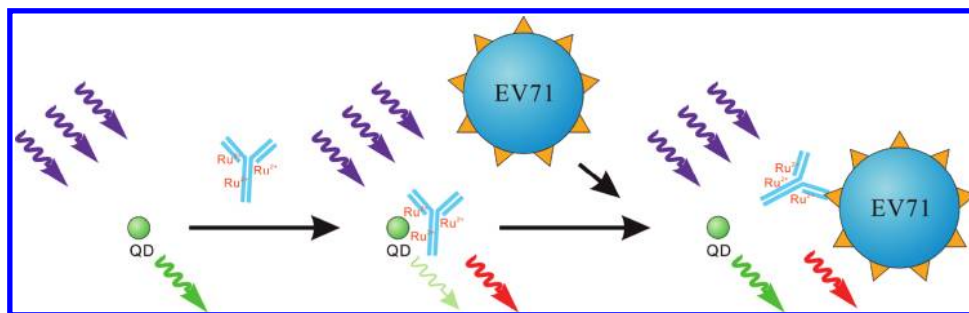
However, among those virus biosensors, sophisticated chips or equipments are designed and detection performance usually requires professional operators and tedious steps, which usually limits their usage. To develop relatively simple homogeneous virus biosensors, fluorescent and colorimetric detection models with the signal output by straightforward color changes are promising.

To construct convenient and sensitive fluorescent and colorimetric virus biosensors, a dual color detection model is adopted due to the high resolution by naked eyes toward a different color change compared to a single fluorescence intensity variation. Therefore, the choice of two fluorescent materials is critical. They are required to be excited at the same single wavelength and emit two different stable and contrasting colors. QDs have always been a popular choice for such a dual color detection model design due to their distinguished optical features such as broad excitation spectra, photo bleaching resistance, and narrow, symmetric, and tunable emission spectra.[14] In the past decades, QDs have been employed in developing dual color based oxygen biosensors.[15,16] However, these oxygen biosensors take CdTe QDs as the reference color whose stability and toxicity are still controversial. So a more stable and environmental friendly fluorescent material will substitute QDs to act as a reference color. To the best of our knowledge, ruthenium complex can be a good alternative to solve this problem. It has the excitation and emission wavelengths at around 450 and 610 nm, respectively.[17] It can provide very stable fluorescence intensity with repeated excitation and more importantly, the ruthenium complex and QDs could be excited at the same wavelength and emit different colors, serving as a good pair of dual color biosensor materials for strategy design. However, before our biosensor design, it is significant to consider the QDs toxicity problem. In our previous work, we have successfully synthesized a series of water-soluble CdTe QDs with different fluorescence emission wavelengths and high PL quantum efficiencies.[18,19] Although these QDs have very excellent optical features, they still have some drawbacks including release of toxic Cd^{2+} to the environment. Intravenous injection of such CdTe QDs to mice will lead to rapid accumulation in the liver and peripheral regions.[20] Maysinger et al. reported that both uncoated and ZnS coated CdTe QDs could induce the accumulation of Cd^{2+}.[21] So great efforts have been endeavored to search for lower toxic metals such as Zn^{2+} during QDs preparation. Until now, we have successfully synthesized a series of high-quality CdTe:Zn^{2+} QDs with very excellent PL quantum efficiency and lower toxicity. By taking advantage of these lower toxicity QDs, a series of environment friendly biosensors can be developed, such as in DNA, protein, and virus

detection as well as dual color fluorescent biosensors.[22−24] Our group has taken advantage of QDs and the ruthenium complex in developing a dsDNA biosensor. The ruthenium complex on one hand can serve as a quencher to QDs fluorescence and on the other hand can bind strongly with dsDNA, and on the basis of this quencher tether ligand (QTL) model, dual-color fluorescence detection of dsDNA can be accomplished by the QD-ruthenium complex dyads, performing in a signal-on fashion.[25] Unfortunately, the dsDNA biosensor can neither distinguish different DNA sequences nor be applied in detecting protein or virus due to the limitation of $Ru(bpy)_2(dppx)^{2+}$, which is called the DNA molecular "light switch".[26] Inspired by this design strategy and to solve the limitation problem, $Ru(bpy)_2(mcbpy-O-Su-ester)(PF_6)_2$ was employed in our detection design and EV71 was selected as a model analyte to illustrate our design strategy. EV71 monoantibody was easily covalently coupled with $Ru(bpy)_2(mcbpy-O-Su-ester)(PF_6)_2$ to form a stable complex Ru-Ab, which also acted as the effect quencher of QDs fluorescence and meanwhile the capture probe of virus antigen EV71. The target EV71 can break up the low fluorescent ionic ensemble by antigen−antibody combination to set free the fluorescent QDs and restore the fluorescence of them whereas the fluorescence intensity of Ru-Ab keeps constant. The Ru complex is a better internal fluorescent reference than QDs in the literature due to its good stability. Therefore, the sensor could not only achieve rapid and precise quantitative determination of EV71 by fluorescence intensity but also could be applied in semiquantitative EV71 determination by digital visualization. This strategy can be used as a universal sensor for any protein/virus by changing the antibodies in disease early diagnosis and provides a fast, simple, and promising clinical approach for virus determination by a dual color change signal that can be identified by the naked eye. The detection strategy design is illustrated in Scheme 1.

■ EXPERIMENTAL SECTION

Material and Reagents. Sodium phosphate monobasic dihydrate ($NaH_2PO_4 \cdot 2H_2O$), sodium phosphate dibasic dodecahydrate ($Na_2HPO_4 \cdot 12H_2O$), sodium chloride (NaCl), bis-(2,2′-bispyridine)-4′-methyl-4-carboxy bipyridine-ruthenium N-succinimidyl ester-bis (hexafluorophosphate) ($C_{36}H_{29}F_{12}N_7O_4$-P_2Ru), and N-acetylcysteme (NAC) were commercially available from Sigma (St. Louis, MO). Tellurium (reagent powder), $CdCl_2 \cdot 2.5H_2O$, $ZnCl_2$, and sodium borohydride ($NaBH_4$) were obtained from Sinopharm Chemical Reagent and were used as capping agents without additional purification. All chemicals used were of analytical grade or of the highest

purity available. All solutions were prepared using Milli-Q water (Millipore) as the solvent.

Synthesis of QDs. In a typical synthesis, sodium borohydride (20 mg) was reacted with tellurium powder (25 mg) in deionized water (1.0 mL) to produce sodium hydrogen tellurium (NaHTe). The mixture of Zn^{2+}-NAC and Cd^{2+}-NAC was prepared by dissolving $CdCl_2 \cdot 2.5H_2O$, $ZnCl_2$, and NAC in deionized water and adjusting the pH to 9.0 by dropwise addition of NaOH solution (1 M). The fresh NaHTe solution (0.4 mL) was then injected into a N_2-saturated mixture of Zn^{2+}-NAC and Cd^{2+}-NAC precursor solution under vigorous stirring. The typical molar ratio of Cd, Zn, Te, and NAC introduced was 1:2:0.2:3.6 in a total volume of 40 mL with 6.25 mM of Cd^{2+} concentration. A volume of 40 mL of precursor was put into a Teflon-lined stainless steel autoclave with a volume of 50 mL. The autoclaves were maintained at the desired growth temperature (200 °C). Each autoclave was cooled to room temperature at regular time intervals after the initial heating.

To remove NAC-Cd/Zn complex at the end of the synthesis, cold 2-propanol was added to the reaction mixture to precipitate NAC-capped CdTe:Zn^{2+} QDs. The as-prepared products were dried overnight under vacuum at 40 °C for further experiments.

Preparation of Ru-Ab Conjugates. The coupled procedure was followed by the commercial protocols. Briefly, 50 μg of antibody was dissolved in 500 μL of PBS (10 mM sodium phosphate and 10 mM NaCl pH 8.0) along with 1 mg of $Ru(bpy)_2(mcbpy-O-Su-ester)(PF_6)_2$ and incubated 30 min at room temperature with continuous agitation. Labeled Ru-Ab was purified by ultra-filtration with a 50K ultrafiltration tube with rotation at 8000g for 10 min and reverse ultrafiltration at 2000g for 5 min. This step was repeated for at least three times. Labeled Ru-Ab concentration was determined using the Ru UV—vis absorbance at 460 nm. Purified Ru-Ab was lyophilized and stored at 4 °C until use.

Cell Culture and Virus Propagation. Vero cells (African green monkey kidney cells) and RD (rhabdomyosarcoma) cells were maintained in mediums according to the instructions of the American Type Culture Collection. The EV71 BrCr TR strain (obtained courtesy of Institute of Biomedical Engineering, Chinese Academy of Medical Sciences and Peking Union Medical Colloge) was propagated in 80—90% confluent monolayers of Vero cells. Briefly, virus stocks were prepared from infected cell cultures displaying typical cytopathic effects (CPE) by three sequential freeze—thaw cycles between —80 and 37 °C, with cellular debris removed by centrifugation at 3 000g for 15 min and then filtration through 0.22 μm sterile membranes. Virus titers were determined as the tissue culture infectious dose ($TCID_{50}$) in RD cells using the Reed-Muench formula.

Apparatus and Procedures. UV—vis absorption spectra data were recorded by a UV-2550 spectrophotometer (Shimadzu, Tokyo, Japan). Fluorescence spectra data were collected with a RF-5301PC fluorescence spectrophotometer (Shimadzu, Tokyo, Japan). Fluorescence intensity decay curves were measured on a FELIX32 system (Photon Technology International). The sensor was put in a ZF-20D black-box type UV analyzer (Shanghai electro-optical instrument factory), and the fluorescent photos were taken by a digital camera. Samples containing appropriate concentrations of Ru-Ab, CdTe:Zn^{2+} QDs, and EV71 were made up to 0.6 mL in 15 mM PBS buffer solution (pH 8.0, 15 mM NaCl). The fluorescence emission spectrum of the solution was then measured 15 min later. All optical measurements were performed at room temperature under ambient conditions, and the excitation wavelength (λex) was 460 nm.
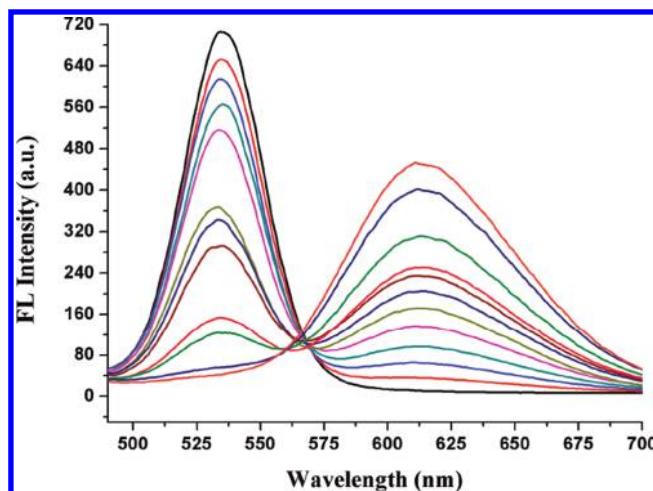

Figure 1. Changes in the fluorescence spectra of NAC-capped CdTe:Zn^{2+} QDs (32 nM) in 15 mM PBS solution (pH 8.0; λex = 460 nm) with an increasing concentration of Ru-Ab, with concentrations of 0, 0.28, 0.5, 0.76, 1.0, 1.85, 2.16, 2.7, 3.24, 3.78, 4.32, and 4.86 nM (from top to bottom).

■ RESULTS AND DISCUSSION

Ru-Ab As an Excellent Quencher to QDs Fluorescence and a Stable Red Color Fluorescent Reference. In our previous work, Ru complex has been used as a quencher of QDs fluorescence to develop a dsDNA sensor.[27] In the determination of dsDNA, the fluorescence of CdTe QDs and Ru complex increase simultaneously. In order to develop a novel, dual color, more precise, and environmental friendly method, water-soluble CdTe:Zn^{2+} QDs were synthesized by the literature known as the hydrothermal process[28,29] and mixed with Ru-Ab complex to form the immune ensemble probe. To make room for dual color detection, green fluorescent CdTe:Zn^{2+}QDs with an emission peak at 533 nm were purposely chosen for our investigation. The fluorescence spectrum of QDs does not overlap with the excitation spectra of Ru complex (Figures S1 and S2 in the Supporting Information). So we speculate the quenching mechanism of the Ru-Ab complex to QDs fluorescence could not be energy transfer. To investigate the possible mechanism of the Ru-Ab complex quenching QDs fluorescence, the fluorescence intensity decay lifetime and UV—vis spectra were collected to illustrate the possible mechanism. Mean fluorescent decay lifetime of QDs and the immune ensemble probe of QDs and Ru-Ab were 22.5 and 22.6 ns, respectively, indicating that ground state complex formation may be the quenching mechanism (Figure S3 in the Supporting Information). Also, the UV—vis spectra change also suggested that the possible interaction mechanism between QDs and Ru-Ab might be static quenching, and they could form a stable ground state complex (Figure S4 in the Supporting Information). Therefore, we investigated quenching behavior by using the conventional static quenching relationship:[30]

$$\lg(F_0 - F)/F = \lg K_A + n \lg C_Q \qquad (1)$$

where F_0 and F are the fluorescence intensities of QDs in the absence and presence of Ru-Ab, respectively; C_Q is the concentration of Ru-Ab; K_A is the ground state complex formed constant, and n is the binding sites. The relationship between $\lg(F_0 - F)/F$ and the concentration of Ru-Ab demonstrate the highly efficient quenching produced by the Ru-Ab. From a plot of $\lg(F_0 - F)/F$
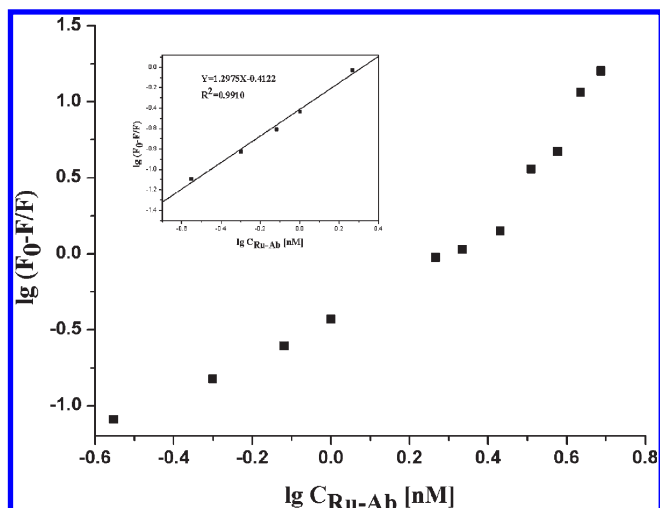
Figure 2. Static quenching plot of NAC-capped CdTe:Zn^{2+} QDs fluorescence quenched by Ru-Ab in 15 mM PBS buffer solutions.

versus lg C_Q, the binding constant of Ru-Ab with QDs (K_A) and the binding sites (n) can be obtained from the intercept and the slope. As shown in Figures 1 and 2, the linear range is 0.28–1.85 nM, K_A is 3.86×10^8 M^{-1}, and n is about 1.30, indicating Ru-Ab is an excellent quencher to QDs fluorescence. Notably, the dual fluorescence emission peaks performed by Ru-Ab quenching QDs fluorescence are due to the broad absorption spectra of QDs. As Ru-Ab fluorescence, intensity is relatively low when excited at λex = 388 nm, resulting in its emission peaks not distinguished clearly with the increased concentration of Ru-Ab. So all the fluorescence data are collected with λex = 460 nm, which is the Ru-Ab maximum absorption wavelength and meanwhile suitable for excitation of QDs. In this method, the green-colored QDs and red-colored Ru-Ab could form the immune ensemble probe. The target EV71 can break up the low fluorescent ionic ensemble by an antigen–antibody combination to set free the fluorescent QDs and restore the fluorescence of them, whereas the fluorescence intensity of Ru-Ab keeps constant. So the Ru complex is a better internal fluorescent reference than the QDs reported.[15]

Interactions between the Ru-Ab Complex and EV71. Ru-(bpy)$_2$(mcbpy-O-Su-ester)(PF$_6$)$_2$ was utilized in our virus biosensor design for two sound reasons. On one hand, it can efficiently quench the fluorescence of CdTe:Zn^{2+} QDs. On the other hand, it also serves as a label to bind any protein such as antibody to be an internal fluorescent reference. Because of the strong and specific binding of antibody with the target EV71, EV71 can break up the low fluorescent QD-Ru-Ab ground state complex and set free the fluorescent QDs enabling them to display the first signal output at 533 nm in signifying the binding event. With this detection model, we can selectively and specifically detect target EV71. More importantly, this model strategy can expand its application to any protein or virus of interest as long as there are suitable antibody–antigen pairs. Therefore, the detection strategy can be employed as a universal detection strategy in the homogeneous aqueous fluorescent immune assay.

As we know, antibody–antigen binding is one of the strongest specific interactions in nature. However, when antibody is labeled with other signal display molecular such as Ru complex, evidence is definitely needed to prove that if there is any negative influence upon the antigen–antibody binding ability. It is worthwhile to
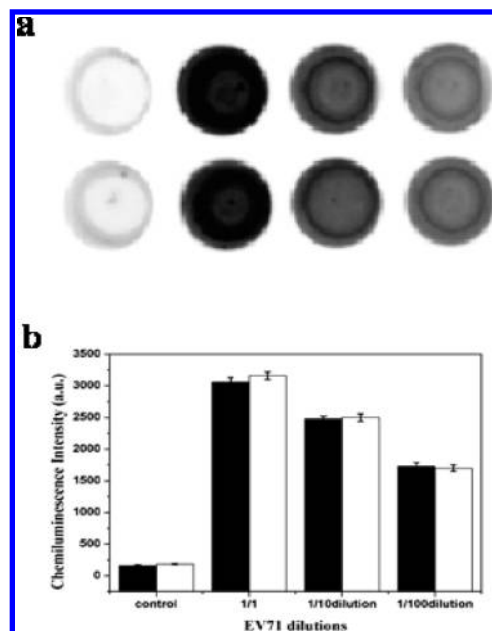

Figure 3. Chemiluminescence images (a) and chemiluminescence intensities (b) of ELISA results by native EV71 Ab and Ru labeled Ab.
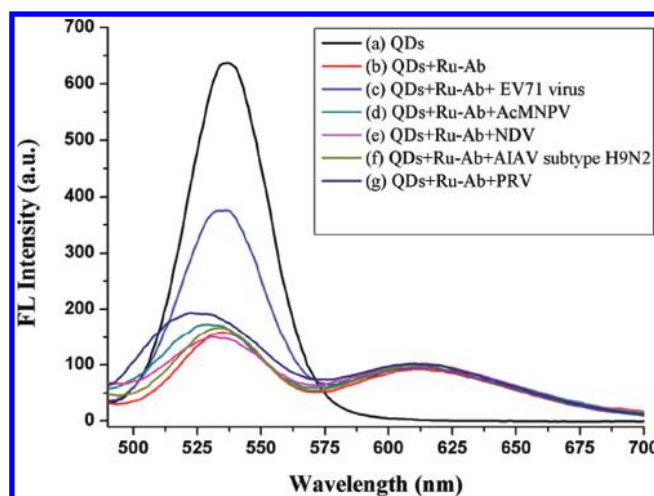

Figure 4. Fluorescence spectra of QDs (a), QDs and Ru-Ab (b), QDs, Ru-Ab and EV71(c), QDs, Ru-Ab and *Autographa californica* nucleopolyhedrovirus(AcMNPV) (d), QDs, Ru-Ab, and Newcastle disease virus (NDV) (e), QDs, Ru-Ab, and Avian influenza-A virus (AIAV) subtype H9N2 (f), QDs, Ru-Ab, and Pseudorabies virus (PRV) (g). QDs, 32nM; Ru-Ab, 0.4 nM; EV71, 380 ng/mL; AcMNPV, NDV, AIAV subtype H9N2, and PRV, 5, 6.2, 4.6, and 3.5 μg/mL, respectively.

investigate the binding ability between Ru-Ab and antigen compared to native antibody and antigen. Therefore, a traditional ELISA experiment is performed by comparing horseradish peroxidase (HRP) labeled secondary antibody to catalyze the luminol and hydrogen-peroxide chemiluminescence. Our ELISA experiment results indicate that the labeled antibody has the same binding ability as the native antibody (Figure 3). Therefore, we can use the Ru-Ab in our homogeneous aqueous immune assay without these concerns. Meanwhile, we investigated the Ru-Ab specific interaction ability with its target by comparing with other viruses. As shown in Figure 4 we found that there was very good

selectivity of labeled antibody to its target EV71. Other viruses could not recover the quenched fluorescence of QDs.

Novel QDs Based Biosensor for Dual Color Determination of EV71. After the proposed sensing strategy has been validated with EV71, we begin to fine-tune the measuring conditions to optimize the sensitivity and selectivity of the sensory device. Since the fluorescence of CdTe:Zn^{2+} QDs is very sensitively affected by pH, the effect of pH of the QDs solution on the fluorescence intensity was studied and the results are shown in Figure S5 in the Supporting Information. If the pH varies from 3.0 to 6.0, the fluorescence intensity of CdTe:Zn^{2+} QDs is very low; when the pH varies from pH 7.0 to 10.0, the QDs fluorescence intensity is high enough to act as a very good signal display unit. Maximum relative fluorescence intensity occurs at pH 8.0. The reasons may be explained as follows: first, the −SH easily falls off in an acidic environment due to the presence of H$^+$. Second, lattice defects in QDs usually happen in acidic conditions. Both the two reasons caused the QDs fluorescence intensity to decrease or even disappear. Therefore, all steps should be conducted in pH 8.0 PBS buffer to obtain stable and strong fluorescence from QDs. In practical experiments, we found the concentration of PBS also greatly influenced the binding ability between Ru-Ab and EV71. Because EV71 as a virus must keep its three-dimensional structure, a certain amount of salt is required. The salt concentration must be suitable for the virus being, and only whereby the EV71 is in its most natural structure can it bind with antibody with a high binding constant. Therefore, we optimized the PBS concentrations before the detection experiment. It was found that 15 mM was the most suitable concentration for fluorescence signal display (Figure S6 in the Supporting Information).

To the best of our knowledge, proteins such as BSA can nonspecifically bind with QDs and usually cause enhancement of QDs fluorescence intensity. These phenomena would result in a false positive of signal output. To avoid the influence of other proteins, BSA was selected as an example to investigate the protein effect on the detection system. First, the enhancement of the fluorescence intensity of QDs by BSA at different concentrations was investigated; as shown in Figure S7 in the Supporting Information when BSA concentrations varied from 10 to 250 μg/mL, an obvious fluorescence enhancement was obtained. Second, the same concentration range of BSA was added into the mixture solution of QDs and Ru-Ab; as it can be seen, the quenched fluorescence intensity was kept almost constant but higher than that in the absence of BSA. Finally, we investigated the fluorescence recovered in the presence of the same concentration of BSA, and as also shown in Figure S7 in the Supporting Information, the ΔF was the same as that in the absence of BSA. Therefore, we think that a certain amount of BSA could not interrupt our detection system. On the other hand, EV71 itself has capsid protein, and it is necessary to study the influence of EV71 on fluorescence intensity of QDs. As shown in Figures S8 and S9 in the Supporting Information, EV71 slightly enhanced the fluorescence of QDs in PBS buffer solution and rarely enhanced the fluorescence of QDs in PBS buffer solution containing 160 μg/mL BSA. This may be due to the protection effect of BSA on QDs by nonspecific interactions. So we carried out EV71 determination in PBS buffer solution containing 160 μg/mL BSA. As shown in Figures 5 and 6, the detection limit of the EV71 in PBS solution is 0.64 ng/mL with a linear range 1.8−210 ng/mL, whereas the detection limit of EV71 in buffer solution contained 160 μg/mL BSA is 0.67 ng/mL with a
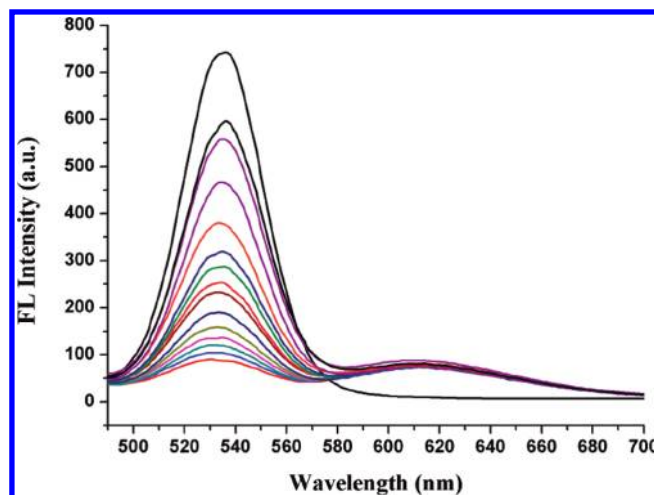

Figure 5. Fluorescent spectra of 32 nM NAC-capped CdTe:Zn^{2+} QDs and 2.5 nM Ru-Ab in the presence of EV71 with concentrations of 0, 1.8, 30, 60, 90, 140, 210, 400, 600, 1 000, 2 000, 6 000, 10 000, and 12 000 ng/mL (from bottom to top). Excitation wavelength: 460 nm.
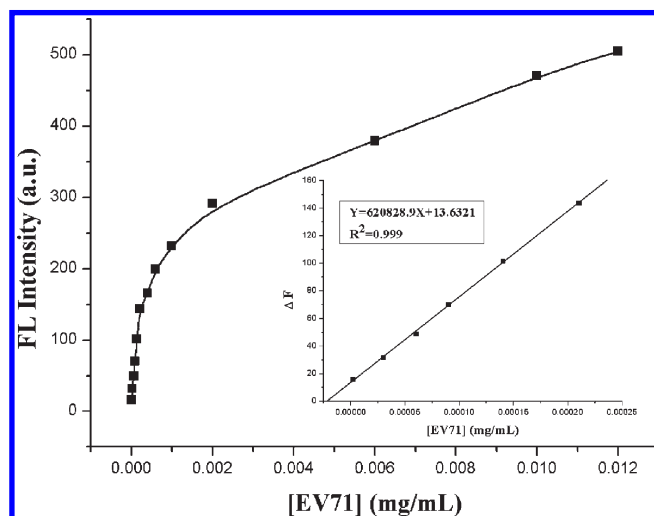

Figure 6. Calibration curve of the NAC-capped CdTe:Zn^{2+} QDs and the Ru-Ab based EV71 biosensor (inset, linear relationship between the relative fluorescence increase intensity and the EV71 concentration). Experimental conditions: 32 nM NAC-capped CdTe:Zn^{2+} QDs and 2.5 nM Ru-Ab in the presence of EV71 with concentrations of 0, 1.8, 30, 60, 90, 140, 210, 400, 600, 1 000, 2 000, 6 000, 10 000, and 12 000 ng/mL. Excitation wavelength: 460 nm.

linear range of 1.8−140 ng/mL (Figure 7). It is notable that virus concentration can also be evaluated by the ratio of the QDs green-colored fluorescence peak intensity to the Ru-Ab red-colored fluorescence peak intensity without the need for a calibration curve, as the Ru-Ab fluorescence intensity is constant whereas the QDs fluorescence intensity increased with the increasing concentration of virus. When the ratio is 1−2 times, it indicates that the virus is about 1.8−90 ng/mL, and when the multiple is beyond 7 times it indicates that the virus is more than 10 μg/mL. In this system, a visualization virus determination is easily realized. The green-colored QDs and red-colored Ru-Ab could form the immune ensemble probe. The fluorescence intensity of the red-color Ru-Ab complex keeps constant, and
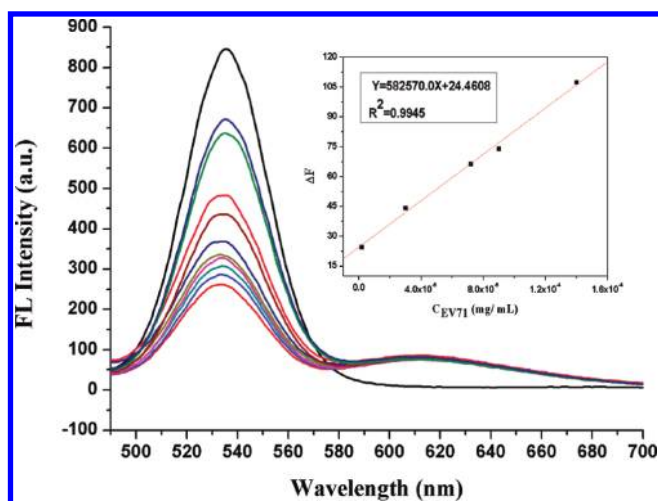
Figure 7. Fluorescence spectra and calibration curve (inset) of 32 nM NAC-capped CdTe:Zn^{2+} QDs and 2.5 nM Ru-Ab in the presence of different concentrations of EV71 in 15 mM PBS buffer solution containing 160 μg/mL BSA. Excitation wavelength: 460 nm.
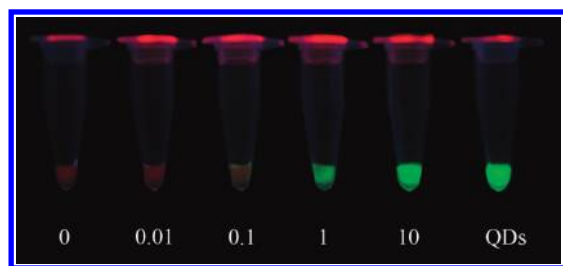

Figure 8. Visualization photos of semiquantitative determination of EV71. The concentration of EV71 are 0, 0.01, 0.1, 1, and 10 μg/mL, respectively (from left to right, the last one is QDs solution as the contrast).

Table 1. Analytical Results for the Determination of EV71 in Human Throat Swab Clinical Samples

	added (ng/mL)	found (ng/mL)	mean recovery (%)	RSD (%) (n = 3)
sample 1	0	20.00 ± 0.08		2.6
	20	40.70 ± 0.05	101.7	1.8
	40	59.80 ± 0.02	99.6	0.9
	60	78.90 ± 0.06	98.6	0.5
sample 2	0	6.00 ± 0.02		2.1
	20	25.60 ± 0.04	98.4	1.2
	40	46.20 ± 0.06	100.4	0.8
	60	65.30 ± 0.03	98.9	0.3
sample 3	0	5.40 ± 0.02		2.0
	20	26.12 ± 0.04	102.8	0.5
	40	44.09 ± 0.02	97.1	1.0
	60	66.07 ± 0.08	101.1	0.3
sample 4	0	17.06 ± 0.04		2.8
	20	38.21 ± 0.05	103.1	1.7
	40	57.90 ± 0.03	101.7	2.5
	60	76.35 ± 0.02	98.9	1.8
sample 5	0	51.24 ± 0.05		1.6
	20	70.80 ± 0.06	99.38	3.6
	40	92.07 ± 0.02	100.9	2.4
	60	112.83 ± 0.08	100.4	0.9
sample 6	0	12.38 ± 0.03		2.5
	20	32.56 ± 0.05	100.55	2.4
	40	52.35 ± 0.06	99.9	0.8
	60	71.93 ± 0.02	99.4	1.2
sample 7	0	34.24 ± 0.05		1.4
	20	54.21 ± 0.06	99.9	2.8
	40	75.02 ± 0.05	101.1	0.8
	60	94.87 ± 0.04	100.7	1.5

the fluorescence intensity of green-color QDs is very sensitive to the change of the amount of EV71. It was found that 10 ng/mL–10 μg/mL EV71 can be detected visually (Figure 8).

Application to Clinical Sample Analysis. We also demonstrated that this homogeneous immune detection strategy could be applied to detect human throat swabs as clinical samples obtained from EV71 positive cases. (See in the Supporting Information for the clinical sample preparation protocol). The analytical results for the clinical samples spiked with 20–60 ng/mL are given in Table 1. The concentrations of EV71 virions in the spiked clinical samples determined by the developed method were in good agreement with those of EV71 viral particles added, along with the quantitative recovery from 98.4% to 101.7%, demonstrating the potential clinical applicability of the Ru-Ab immunofluorescent sensor based on water-soluble CdTe:Zn^{2+} QDs and Ru-Ab for the quantification of EV71.

Generality of the CdTe:Zn^{2+} QDs and Ru-Ab Based Biosensor. To verify the generality of the CdTe:Zn^{2+} QDs and Ru-Ab based biosensor for protein determination, mouse IgG was chosen as a model analyte to demonstrate the issue. Goat-antimouse IgG was conjugated with Ru complex to act as the new capture probe, and rabbit IgG was selected as the control target analyte. As shown in Figure S10 in the Supporting Information, mouse IgG can easily recover the fluorescence of QDs and Ru-Ab ensemble whereas rabbit IgG cannot restore the

fluorescence, which has strongly proved that the QDs fluorescence recover is dependent on the antibody−antigen combination and a nonspecific interaction cannot effect the selective immuno interaction. Therefore, mouse IgG can also be quantified by this detection strategy. Figure S11 in the Supporting Information has shown the quantification result, 1.1 ng/mL mouse IgG can be detected by 3 times the signal-to-noise ratio with a linear relationship between 5.0 and 180 ng/mL. The evidence has demonstrated that the strategy can extend to any protein detection by changing the conjugated antibodies as the new capture probe.

■ CONCLUSIONS

A simple, sensitive, highly selective, and rapid QD-based virus sensing ensemble is developed for the detection of EV71 with dual fluorescence output signals. Interferences caused by BSA and other viruses for detection are minimal. Apparently, the sensor has good potential to expand its application to the early diagnosis determination of any virus by changing antibodies. According to the proposed sensing strategy, chemical modification on both the QDs and target molecules is not required. It can be applied in real sample analysis with a satisfactory result obtained. This optical sensor could not only achieve rapid and precise quantitative determination of protein/virus by

fluorescent intensity but also could be applied in semiquantitative protein/virus determination by digital visualization. Exploitation of the present sensory system to other virus detection and high-throughput screening of virus subtypes will be undertaken.

■ ASSOCIATED CONTENT

ⓢ Supporting Information. Additional information as noted in text. This material is available free of charge via the Internet at http://pubs.acs.org.

■ AUTHOR INFORMATION

Corresponding Author
*Phone: (+86)-27-68756557. Fax: (+86)-27-68754067. E-mail: zhkhe@whu.edu.cn.

■ ACKNOWLEDGMENT

■ REFERENCES

(1) Han, J. F.; Cao, R. Y.; Jiang, T.; Yu, M.; Liu, W.; Tian, X.; Qin, E. D.; Cao, W. C.; Qin, C. F. *J. Clin. Virol.* **2011**, *50*, 348–349.

(2) Liu, L. D.; Zhao, H. L.; Zhang, Y.; Wang, J. J.; Che, Y. C.; Dong, C. H.; Zhang, X. M.; Na, R. X.; Shi, H. J.; Jiang, L.; Wang, L. C.; Xie, Z. P.; Cui, P. F.; Xiong, X. L.; Liao, Y.; Zhao, S. D.; Gao, J. H.; Tang, D. H.; Li, Q. H. *Virology* **2011**, *412*, 91–100.

(3) Park, J. S.; Cho, M. K.; Lee, E. J.; Ahn, K. Y.; Lee, K. E.; Jung, J. H.; Cho, Y. J.; Han, S. S.; Kim, Y. K.; Lee, J. *Nat. Nanotechnol.* **2009**, *4*, 259–264.

(4) Holopainen, R.; Honkanen, J.; Jensen, B. B.; Ariel, E.; Tapiovaara, H. *J. Virol. Methods* **2011**, *171*, 225–233.

(5) Papillard-Marechal, S.; Enouf, V.; Schnuriger, A.; Vabret, A.; Macheras, E.; Rameix-Welti, M. A.; Page, B.; Freymuth, F.; Vander-Werf, S.; Garbag-Chenon, A.; Chevallier, B.; Gaillard, J. L.; Gault, E. *J. Med. Virol.* **2011**, *83*, 695–701.

(6) Horwood, P. F.; Mahony, T. J. *J. Virol. Methods* **2011**, *171*, 360–363.

(7) Puttikhunt, C.; Prommool, T.; U-thainual, N.; Ong-Ajchaowlerd, P.; Yoosook, K.; Tawilert, C.; Duangchinda, T.; Jairangsri, A.; Tangthawornchaikul, N.; Malasit, P.; Kasinrerk, W. *J. Clin. Virol.* **2011**, *50*, 314–319.

(8) Shahsavandi, S.; Salmanian, A. H.; Ghorashi, S. A.; Masoudi, S.; Fotouhi, F.; Ebrahimi, M. M. *J. Virol. Methods* **2011**, *171*, 260–263.

(9) Fleischmann, A.; Schlomm, T.; Kollermann, J.; Sekulic, N.; Huland, H.; Mirlacher, M.; Sauter, G.; Simon, R.; Erbersdobler, A. *Prostate* **2009**, *69*, 976–981.

(10) Koene, G. J. P. A.; Arts-Hilkes, Y. H. A.; Van-Dijk, A. J. G.; Vander-Ven, K. J. W.; Slootweg, P. J.; De-Weger, R. A.; Tilanus, M. G. J. *Hum. Immunol.* **2004**, *65*, 1455–1462.

(11) Gafka, A. C.; Vogel, K. S.; Linn, C. L. *Neuroscience* **1999**, *90*, 1403–1414.

(12) Gerasimov, J. Y.; Lai, R. Y. *Chem. Commun.* **2010**, *46*, 395–397.

(13) Yanik, A. A.; Huang, M.; Kamohara, O.; Artar, A.; Geisbert, T. W.; Connor, J. H.; Altug, H. *Nano Lett.* **2010**, *10*, 4962–4969.

(14) Mei, B. C.; Susumu, K.; Medintz, I. L.; Mattoussi, H. *Nat. Protoc.* **2009**, *4*, 412–423.

(15) Wang, X. D.; Chen, X.; Xie, Z. X.; Wang, X. R. *Angew. Chem., Int. Ed.* **2008**, *47*, 7450–7453.

(16) Wang, X. D.; Meier, R. J.; Link, M.; Wolfbeis, O. S. *Angew. Chem., Int. Ed.* **2010**, *49*, 4907–4909.

(17) Fernandez-Moreira, V.; Thorp-Greenwood, F. L.; Coogan, M. P. *Chem. Commun.* **2010**, *46*, 186–202.

(18) Zhao, D.; He, Z. K.; Chan, P. S.; Wong, R. N. S.; Mak, N. K.; Lee, A. W. M.; Chan, W. H. *J. Phys. Chem. C* **2010**, *114*, 6216–6221.

(19) Zhao, D.; He, Z. K.; Chan, W. H.; Choi, M. M. F. *J. Phys. Chem. C* **2009**, *113*, 1293–1300.

(20) Chu, M. Q.; Wu, Q.; Wang, J. X.; Hou, S. K.; Miao, Y.; Peng, J. L.; Sun, Y. *Nanotechnology* **2007**, *18*, 1–6.

(21) Sandros, M. G.; Behrendt, M.; Maysinger, D.; Tabrizian, M. *Adv. Funct. Mater.* **2007**, *17*, 3724–3730.

(22) Kim, J. U.; Lee, M. H.; Yang, H. *Nanotechnology* **2008**, *19*, 1–5.

(23) Zou, W. S.; Sheng, D.; Ge, X.; Qiao, J. Q.; Lian, H. Z. *Anal. Chem.* **2011**, *83*, 30–37.

(24) Liu, J. X.; Chen, H.; Lin, Z.; Lin, J. M. *Anal. Chem.* **2010**, *82*, 7380–7386.

(25) Zhao, D.; Chan, W. H.; He, Z. K.; Qiu, T. *Anal. Chem.* **2009**, *81*, 3537–3543.

(26) Hu, L. Z.; Bian, Z.; Li, H. J.; Han, S.; Yuan, Y. L.; Gao, L. X.; Xu, G. B. *Anal. Chem.* **2009**, *81*, 9807–9811.

(27) Yeh, H. Y.; Yates, M. V.; Mulchandania, A.; Chen, W. *Chem. Commun.* **2010**, *46*, 3914–3916.

(28) He, Y.; Lu, H. T.; Sai, L. M.; Su, Y. Y.; Hu, M.; Fan, C. H.; Huang, W.; Wang, L. H. *Adv. Mater.* **2008**, *20*, 3416–3421.

(29) Medintz, I. L.; Farrell, D.; Susumu, K.; Trammell, S. A.; Deschamps, J. R.; Brunel, F. M.; Dawson, P. E.; Mattoussi, H. *Anal. Chem.* **2009**, *81*, 4831–4839.

(30) Zhang, M.; Lv, Q. L.; Yue, N. N.; Wang, H. Y. *Spectrochim. Acta, Part A* **2009**, *72*, 572–576.